Exploration Geophysics, Remote Sensing and Environment XXVIII.2 (2021)

DOI: 10.26345/egrse-018-21-202

ROTATIONAL-TRANSLATIONAL SCALING RELATIONS FROM INDUCED SEISMIC EVENTS – COMPARISON BEFORE AND AFTER AMPLIFICATION CORRECTION

ROTAČNĚ-TRANSLAČNÍ ŠKÁLOVACÍ VZTAHY INDUKOVANÝCH SEISMICKÝCH UDÁLOSTÍ – POROVNÁNÍ PŘED A PO KOREKCI ZESÍLENÍ

Dariusz Nawrocki [1]***, Maciej J. Mendecki*** [1]***, Lesław Teper*** [1]

Abstract

The rotational and translational signals were registered at the Planetarium (“PLA”) station due to mining exploration, localized in the central part of the Upper Silesian Coal Basin. Visual inspection of the data peak values showed that the scaling relation between peak rotational velocity PRV and peak ground acceleration PGA could be expressed by mathematical relation of a power function. Signals were analyzed using the horizontal-to-vertical spectral ratio (HVSR) method, which leads to estimate resonance frequency and amplification level. Estimated amplification factor leads to estimate next regression models of scaling relation, similar expressed by power and linear functions. Comparison of the estimated function coefficients for raw data and data corrected by the amplification factor showed differences in their values which can be considered as proof of impact of the site effect on rotational motion.

Abstrakt

Seismometrické záznamy rotačních a translačních vibrací v důsledku důlních prací byly zaznamenány na stanici Planetarium (PLA) v centrální části Hornoslezské uhelné pánve. Vizuální kontrola zaznamenaných dat ukázala, že škálovací vztah mezi záznamy špičkové hodnoty rotační rychlosti (PRV) a záznamem špičkové hodnoty translačního zrychlení (PGA) může být vyjádřen výkonovou funkcí. Zaznamenané signály byly podrobeny HVSR analýze, která umožňuje určit hodnotu rezonanční frekvence a parametru zesílení. Zjištěné hodnoty parametrů zesílení byly použity pro stanovení teoretických modelů škálovacích vztahů definovaných lineárními a výkonovými funkcemi. Stanovené parametry škálovacího vztahu dosahují různých hodnot pro empirická data a data korigovaná o faktor zesílení. Výše uvedené pozorování dokazuje vliv geologických podpovrchových vrstev na zaznamenané rotační vibrace.

Keywords
HVSR, mining-induced seismicity, rotational ground motion, scaling relations

Klíčová slova
HVSR, indukovaná seismicita, rotační síly, škálovací vztahy

1 Introduction

Rotational ground motion is described by torsion as motion around a vertical axis and rockings – motions around two horizontal axes (Zembaty, 2006). Generally, rotational seismology studied the effects of natural seismicity (e.g., Igel et al., 2007; Lee et al., 2009; Liu et al., 2009; Stupazzini et al., 2009), but the influence of anthropogenic seismicity also has been taken into consideration (e.g., Kalab et al., 2013; Zembaty et al., 2017, Mutke et al., 2020). The relation between rotational motion and site conditions is still poorly documented issue. It is known that the amplification effect and wave resonance in the ground affect the observed translational signals, which cause amplifying translational peak amplitudes. Therefore, we supposed that it amplification change the nature of rotational motions. The amplification coefficient and resonance frequency were estimated using the single-station Nakamura technique (Nakamura, 1989), In terms of the transitional signal ratio, we have used the horizontal-to-vertical spectral ratio (HVSR). It must be noted that rotation in the horizontal axis is of vertical nature, and rotation in the vertical axis is of horizontal nature (Lee and Liang, 2008; Lee and Trifunac, 2009). As a consequence of that fact we have introduced a torsion to rocking spectral ratio (TRSR), in terms of rotational component spectra estimations. It corresponds to the horizontal rotation spectrum to the vertical rotation spectrum (Sbaa et al., 2017). The aim of this paper was to analyze the influence of amplification on the translation and rotational signals produced by various event generated by mining operations and implemented the results into relation between the maximum peak amplitudes of vertical rotational velocity and horizontal translational acceleration, as has been studied by many authors (e.g. Liu et al., 2009; Takeo et al., 2009; Lee et al., 2009; Yin et al., 2016; Sbaa et al., 2017; Mutke et al., 2020). The estimated HVSR/TRSR maxima were used in the peak amplitude corrections to remove the assumed influence of site effects.

2 Site and data characterization

The seismic observations were carried out by a single seismic station, called "PLA", located in the city of Chorzów (Fig. 1a). The station location allowed to registered rotational seismic data from large distance, which was related mostly to the mine exploration conducted by Bielszowice Mine in the Upper Silesian Coal Basin (USCB), Poland. The presented study concerns the site effects; thus, we assumed a three-layered geological model: loose material (subsoil), intermediate layer, and rigid basement. The rigid basement is a Carboniferous coal-bearing formation represented by sandstones, mudstones, and siltstones interbedded with hard coal seams (Teper, 2000, Mendecki et al., 2020). The intermediate layer is represented by the weathered Triassic sandstones built of rigid and loose material

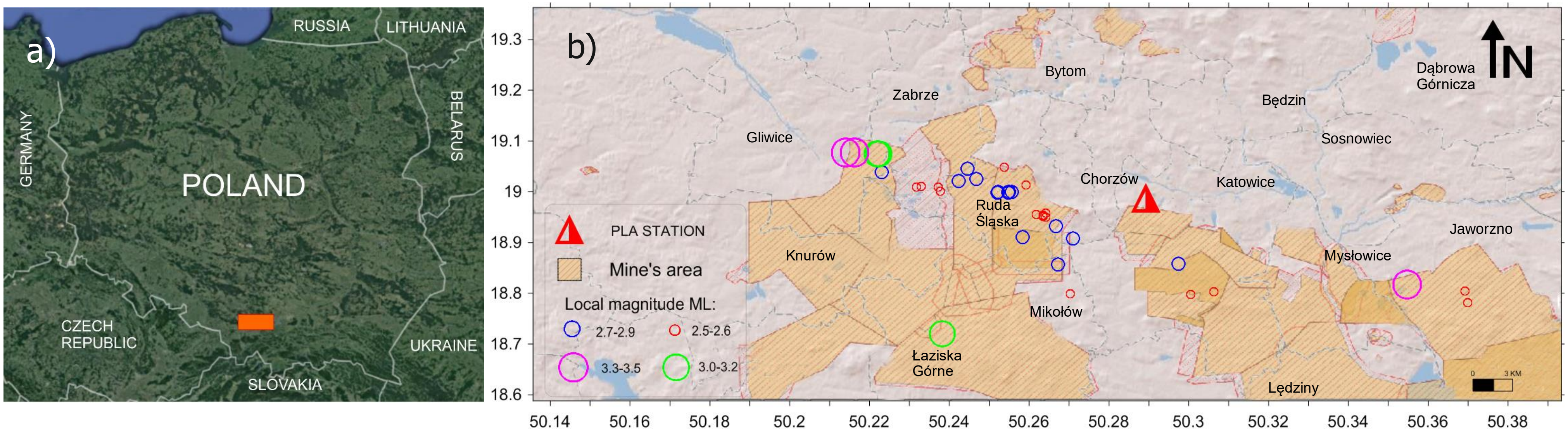

Fig. 1 Study area information: a) sketch of USCB with study area location and b) map of the study area with the seismic event distribution and the PLA station locations

due to the strongly weathered rocks (Buła and Kotas, 1994; Jureczka et al., 1995). The top layer in the vicinity is composed of the Quaternary sediments, represented by mix of: sands, pebbles, muds, alluvia, and peats. (Buła and Kotas, 1994; Jureczka et al., 1995).

The collected seismic data of 46 events (Fig. 1b) were registered by the EENTEC measuring set, composed of the seismic recorder DR-4000 linked to the GPS module, translational seismometer SP-400, translational accelerometer EA-120, and rotational seismometer R-1. SP-400 is a triaxial force-balanced seismometer the dynamic range of which is equal to 142 dB and passband up to 50 Hz. EA-120 is a triaxial force-balanced accelerometer the scale range of which is equal to ± 2g, and the dynamic range is equal to 128 dB. R-1 is a well-known triaxial rotational seismometer which resolution is equal to $1.2x10^{-7} rad/s$ and dynamic range is equal to 110dB, frequency band ranging from 0.05 to 20 Hz, and amplitude clip level of 0.1 rad/s at 1 Hz (www.eentec.com). The Department of Geology and Geophysics, the Central Mining Institute in Katowice, Poland, stores the digital records of seismic events. The strongest of the seismic event, the local

Tab.1 Epicentral distances for the selected energy/magnitude ranges

Energy [J]	**M_L**	**Number**	**Epicentral distance for energy range [km]**
3.55E+05 – 5.50E+06	2.5-2.6	20	5.76 – 20.28
8.51E+06 – 2.04E+07	2.7-2.9	19	5.78-20.43
3.16E+07 – 7.59E+07	3.0-3.2	3	5.93-8.17
1.17E+08 – 2.82E+08	3.3-3.5	3	8.17-9,70

magnitude of which reached M_L 3.5, occurred on June 6, 2016. In the catalog, the local magnitudes of the events range from 2.5 to 3.5 at the distance from 5.7 to 20.4 km (Tab.1). It indicates that relatively large events occurred in distances up to 10 km from the seismic station. Seismic energy values of the events caused high resolution of the rotational seismic signal in combination to the large distance. (see example in Fig. 2)The seismic catalog of the registered events, which contained the data related to the location and energy, was prepared based on the records from the IS-EPOS platform, a unit of the Upper Silesian Geophysical Observation System (Mutke et al., 2019).

3 Methods

3.1 HVSR for translational and rotational signals

The Mining-induced seismic events recorded at a given point (Fig. 3a and Fig. 3c) allow to estimate the HVSR curve, which is formed by the spectral ratio of the horizontal and vertical components. In this analysis, coefficients of the local site effects: the subsurface layer resonance frequency and the amplification were estimated for the S-wave phase from each event. The spectral ratio between the mean horizontal and vertical components was calculated for each event which leads to estimate HVSR curve as the average value all of them (e.g. Bard et al., 2004, Pastén et al., 2015). The HVSR method was transferred to be applicable for rotational signals, which means that ratio of amplification is opposite to the estimated values. It is caused by planes of rotational motion movements. The peak torsion velocity (Fig. 3b) characterizes rotational movements in the horizontal plane, while the peak rocking velocity is the rotation around the horizontal axes (Sbaa et al., 2017). Therefore, HVSR for rotation signals was called by authors: the torsion-to-rocking spectral ratio (TRSR).

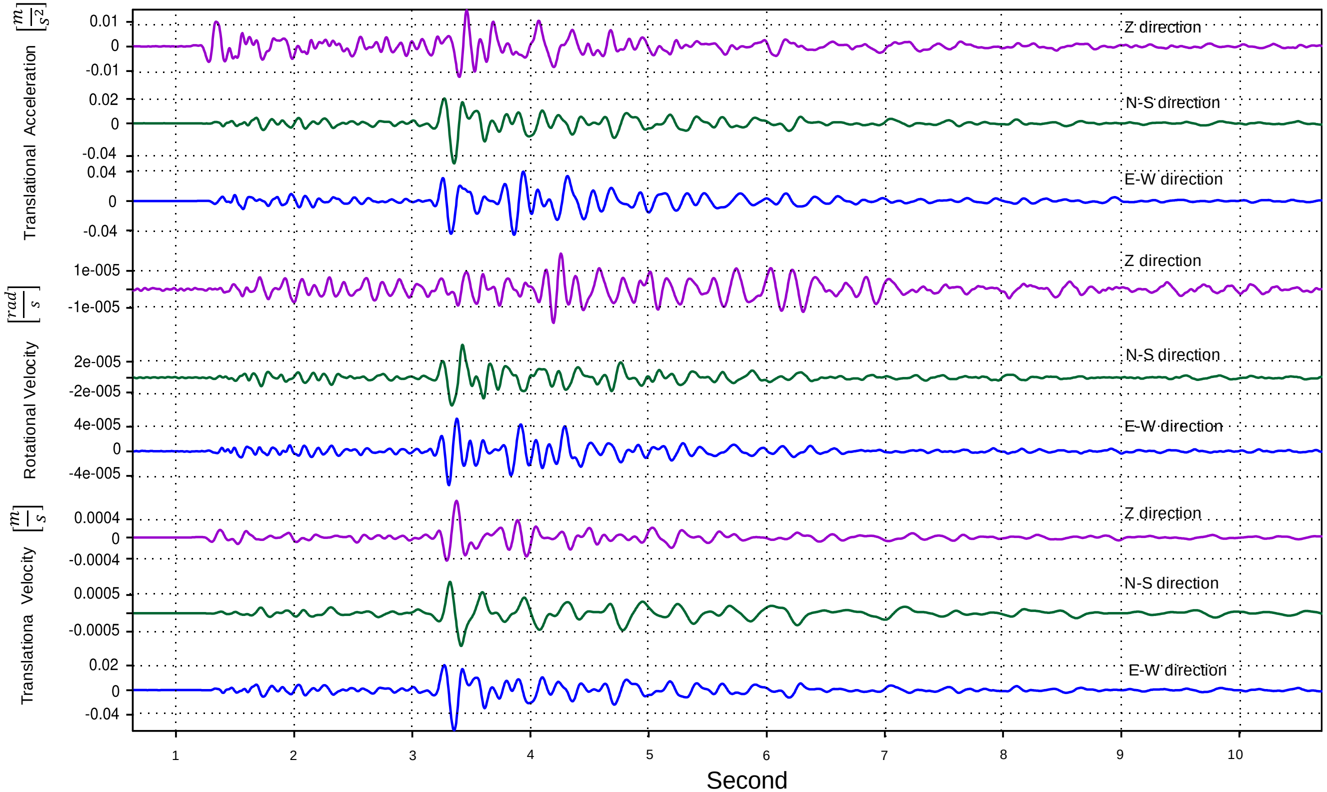

Fig. 2 Seismogram of the seismic event which occurred on June 3, 2016. The local magnitude reached 3.5, and the hypocentral distance was equal to 9.7 km.

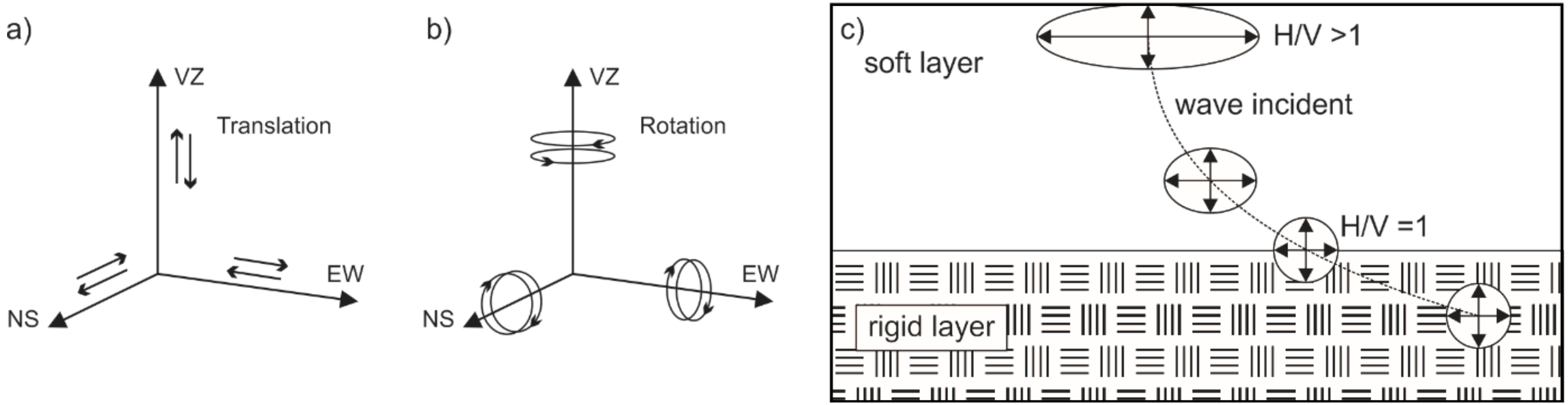

Fig. 3 Motion directions in translation (a) and rotation (b), and an ideal sketch of amplification effectin a soft layer (c)

3.2 Scaling relations

Basing on transverse plane waves, the transverse translation acceleration $\ddot{u}_y(x,t)$ and rotation velocity $\dot{w}_z(x,t)$ are in phase at all times (e.g., Igel et al. 2005), and their ratio is linked to the phase velocity *c*:

$$\frac{\ddot{u}_y(x,t)}{\dot{w}_z(x,t)} = -2c \quad (1)$$

Following the researches (Fichtner and Igel., 2008; Wang., 2008) the plane waves can be replaced by the maximum peak value of the corresponding records: vertical rotational velocity and horizontal translational velocity, and consequently equation (1) can be rewritten as follows:

$$\frac{PGA_H}{PRV_z} = \frac{max\left(\sqrt[2]{a_X^2(t)+a_Y^2(t)}\right)}{PRV_z} = 2c \quad (2)$$

where PGA_H is a horizontal peak ground acceleration, estimated as a root of the sum of squared NS, $a_x(t)$ and EW amplitudes, $a_y(t)$, PRV_z is a vertical peak rotation velocity. The relation (2) was investigated by many authors (e.g., Liu et al., 2009; Takeo et al., 2009; Lee et al., 2009; Yin et al., 2016; Sbaa et al., 2017).Visual inspection of the data applied to the linear regression model of the records convinced us to introduce the power law, thus we rewrote the formulas from equation (2) and supplemented them with power coefficients. Therefore, it can be expressed as follow:

$$PRV_Z = C\left(\sqrt[2]{PGA_X^2 + PGA_Y^2}\right)^D \quad (3)$$

where *C* and *D* are the power-law coefficients.
In order to perform a comparison of the models equation (2) was rewrote as follow:

$$PRV_Z = A \cdot \sqrt[2]{PGA_X^2 + PGA_Y^2} + B \ (4)$$

where *A* and *B* are the linear function coefficients.

4 Results

4.1 HVSR and TRSR

The spectral ratios for all of seismic events were estimated in the same way according to the SESAME criteria (Bard et al., 2004). The analyses were conducted to find the amplification and resonance frequency for average horizontal and EW, and NS directions. The median were calculated from all events (Fig. 4), which allowed to distinguish one general HVSR and TRSR peak (Tab.2). The first maximum was observed at frequency ranging from 3.99 Hz to 4.19 Hz for translation and from 5.6 to 6.0 Hz for rotation.

4.2. Peak rotation and translation scaling relations

Translational peaks representing the horizontal motion were divided by the first value of the HVSR maximum corresponding to amplification. Analogically, peaks of vertical rotational motion were divided by opposite value of averaged first HVSR maximum. Next, the direct data and estimated the regression models were compared. Comparison was performed separately for raw and corrected by amplification factor data. The results of coefficient estimation are presented in Table 3.

Tab.2 Resonance frequencies and amplification factors were obtained for rotation and translation in each component: average, EW (x-axis), and NS (y-axis)

Type of motion	Component	f_0 [Hz]	Peak value
Translation	AV TRSR PGA	3.99	4.44
	EW PGA	4.19	5.49
	NS PGA	4.00	3.49
Rotation	AV HVSR PRV	5.79	1.88
	EW PRV	6.0	2.55
	NS PRV	5.6	1.66

Tab.3 Regression coefficients estimated for the power and linear functions (eq. 3 and 4)

Regression coefficients estimated for the power functions (eq. 3)					
Empirical data/ Corrected data	**C**	**σ(C)**	**D**	**σ(D)**	**R^2**
$PRV_Z = f(PGA_{XY})$	$1.53 \cdot 10^{-4}$	$3.1 \cdot 10^{-5}$	$6.73 \cdot 10^{-1}$	$3.54 \cdot 10^{-2}$	0.89
$PRV_Z = f(PGA_{XY})$	$2.08 \cdot 10^{-4}$	$5.46 \cdot 10^{-5}$	$7.04 \cdot 10^{-1}$	$3.83 \cdot 10^{-2}$	0.88
Regression coefficients estimated for the linear functions (eq. 4)					
Empirical data/ Corrected data	**A**	**σ(A)**	**B**	**σ(B)**	**R^2**
$PRV_Z = f(PGA_{XY})$	$5.07 \cdot 10^{-3}$	$3.07 \cdot 10^{-5}$	$1.59 \cdot 10^{-6}$	$2.69 \cdot 10^{-7}$	0.86
$PRV_Z = f(PGA_{XY})$	$8.36 \cdot 10^{-3}$	$7.20 \cdot 10^{-5}$	$8.49 \cdot 10^{-7}$	$1.95 \cdot 10^{-7}$	0.76

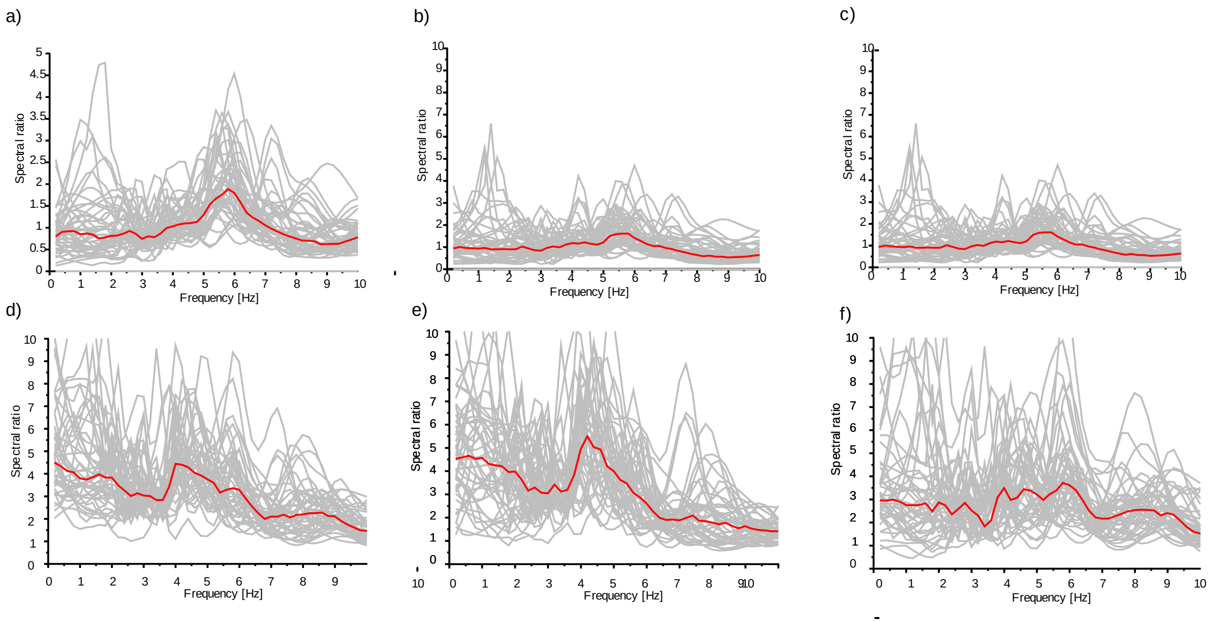

Red line is a median value of cases:
a) average HVSR for rotational velocity;
b) HVSR EW for rotational velocity;
c) HVSR NS for rotational velocity;
d) average HVSR for translational acceleration;
e) HVSR EW for translational acceleration;
f) HVSR NS for translational acceleration.

Fig. 4 HVSR and TRSR curves of 46 events (gray lines)

The values of the standard deviations related to the estimated regression parameters suggested a better fit between empirical data and theoretical equation for power-law than linear relationship (Fig. 5).

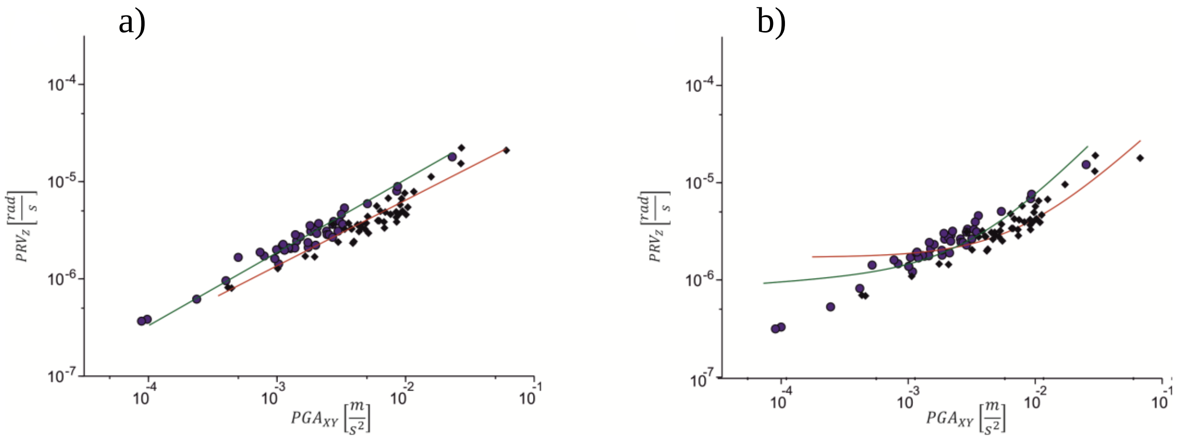

a) power law function
b) linear function

Black and blue dots are data respectively empirical and after amplification correction. Red and green lines are models respectively empirical and after amplification correction.

Fig. 5 Peak rotation-translation scaling relations

5 Discussion

The regression results of estimated linear relation (eq.4) did not provide better results than published (e.g., Liu et al., 2009; Takeo et al., 2009; Lee et al., 2009; Yin et al., 2016; Sbaa et al., 2017). Moreover value of the function coefficients depends on empirical measurements values of rotation and translation motion and as a consequence obligate to estimation different model. Both of the linear function coefficients, “A” and “B” change their values after amplification corrections which suggest affection of the site effect. It is presumed that the unit of the "A" coefficient can be described as $\left[\frac{s}{m}\right]$, while “B” coefficient is unitless or described by $\left[\frac{rad}{s}\right]$. The regression results of estimated power-law relation (eq.3) produced satisfying results. Basing on value of R^2 coefficients, the power-law relation was better approximated than the linear. The impact of the site effect is noticeable as a consequence of increasing values of “C” and “D” coefficients, after amplification correction. It is presumed that the unit of the "C" coefficient can be described as $\left[\frac{s}{m}\right]$, while “D” coefficient is unitless.

6 Conclusion

Translational (HVSR) and rotational (TRSR) ratios indicated different resonance frequency for the first maxima as well as different peak values of TRSR and HVSR. This suggests different values of ground amplification for the rotational and translational motions. The implemented power function as a scaling relation between rotational velocity and translational acceleration peaks produced satisfying regression results. The correction of the amplification peak values had an effect on the estimated values of coefficients "C" and "D" which increased after correction. The linear function, as a scaling relation function produced worse regression results. Although similarly increasing values of the coefficients "A and B" after amplification correction is observable too.

It suggests that all of scaling functions coefficients depends on the local site effect and, thus, can depend to a great extent on the local geology.

Funding

The work on this paper was supported by the Doctoral School at the University of Silesia in Katowice, Poland.

Data and resources

For the catalog of rotational and translational ground motion used in this article, see the Upper Silesian Seismic Network website at http://www.grss.gig.eu/en/a22/Rotational/ (last accessed June 06, 2021). For more information on the R-1, EA-120, and DR-4000 instruments, visit www.eentec.com (last accessed July 07, 2020).

Acknowledgments

The authors would like to thank Profesor Grzegorz Mutke from the Central Mining Institute in Katowice for providing a seismic data with the location of mining seismic events.

References

BARD, P.Y, SESAME participants The SESAME project: an overview and main results. *In: Proceedings, 13th World conference on earthquake engineering*, Paper 2207, 2004.

BUŁA, Z., KOTAS, A. (Eds.) *Geological atlas of the Upper Silesian Coal Basin, part III. Structural-geological maps 1:100 000.* Państwowy Instytut Geologiczny, Warszawa, 1994.

FICHTNER, A., IGEL, H. Sensitivity densities for rotationalground-motion measurements, *Bull. Seismol. Soc. Am.*, 99 (2B), 1302–1314, 2009.

IGEL, H., SCHREIBER, U., FLAWS, A., SCHUBERTH, B., VELIKOSELTSEV, A., COCHARD, A. Rotational motions induced by the M8.1 Tokachi-oki earthquake, September 25, 2003, *Geophys. Res. Lett.*, 32, L08309, 2005, https://doi.org/10.1029/2004GL022336

IGEL, H., COCHARD, A., WASSERMANN, J., SCHREIBER, U., VELIKOSELTSEV, A., PHAM, N.D. Broadband observations of rotational ground motions. *Geophys. J. Int.*,168, 182–197, 2007, https://doi.org/10.1111/j.1365-246X.2006.03146.x.

KALAB, Z., KNEJZLIK, J., LEDNICKA, M. Application of newly developed rotational sensor for monitoring of mining-induced seismic events in the Karvina region. *Acta Geodyn. Geomater.*, 2 (170), 197–205, 2012, https://doi.org/10.13168/AGG.2013.0020.

KONNO, K., OHMACHI, T. Ground-Motion Characteristics Estimated from Spectral Ratio between Horizontal and Vertical Components of Microtremor. *Bull. Seismol. Soc. Am.*, 88 (1), 228-241, 1998.

JURECZKA J., AUST J., BUŁA Z., DOPITA M., ZDANOWSKI A. *Geological map of the Upper Silesian Coal Basin (Carboniferous subcrop)* 1:200 000. Państw. Inst. Geol. Warszawa, 1995.

LEE, W. H. K., HUANG, B.S., LANGSTON, C.A., LIN, C.J., LIU, C.C., SHIN, T.C., TENG, T.L., WU, LEE, V. W., LIANG, L. Rotational components of strong motion earthquakes. *In The 14th World Conference on Earthquake Engineering*, Beijing, 2008.

LEE, V. W., TRIFUNAC, M. D. Empirical scaling of rotational spectra of strong earthquake ground motion. *Bull. Seismol. Soc. Am.*, 99 (2B), 1378-1390, 2009, https://doi.org/10.1785/0120080070

LIU, C. C., HUANG, B.S., LEE, W.H.K., LIN, C.-J. Observing rotational and translational ground motions at the HGSD station in Taiwan from 2007 to 2008. *Bull. Seismol. Soc. Am.*, 99, 1228–1236, 2009, https://doi.org/10.1785/0120080156.

MENDECKI, M. J., SZCZYGIEŁ, J., LIZUREK, G., & TEPER, L. Mining-triggered seismicity governed by a fold hinge zone: The Upper Silesian Coal Basin, *Poland. Eng. Geol.*, 274, 105-728, 2020, https://doi.org/10.1016/j.enggeo.2020.105728

MUTKE, G., KOTYRBA, A., LURKA, A., OLSZEWSKA, D., DYKOWSKI, P., BORKOWSKI, A., ARASZKIEWICZ, A., BARAŃSKI, A. Upper Silesian Geophysical Observation System – A unit of the EPOS project, J. *Sust. Min.*, 18, 198-207., 2019, https://doi.org/10.1016/j.jsm.2019.07.005.

MUTKE, G., LURKA, A., ZEMBATY, Z. Prediction of rotational ground motion for mining-induced seismicity - Case study from Upper Silesian Coal Basin, Poland, 2020, *Eng. Geol.*, 276, 105-767, https://doi.org/10.1016/j.enggeo.2020.105767.

NAKAMURA, Y. A method for dynamic characteristics estimation of subsurface using microtremor on the ground surface. *QR of RTR*, 130, 25-33, 1989.

NAKAMURA, Y. On the H/V spectrum. *The 14th World Conference on Earthquake Engineering*, Beijing, China, 2008.

PASTÉN, C., SÁEZ, M., RUIZ, S., LEYTON, F., SALOMÓN, J., POLI, P Deep Characterization of the Santiago Basin using HVSR and Cross-correlation of Ambient Seismic Noise, *Eng. Geol.*, 201, 57-66, 2015, https://doi: 10.1016/j.enggeo.2015.12.021.

SAROKOLAYI, L.K., BEITOLLAHI, A., ABDOLLAHZADEH, G., AMREIE, S.T.T., KUTANAEI, S.S. Modeling of ground motion rotational components for near-fault and far-fault earthquake according to soil type. *Arab. J. Geosci.*, 8, 3785–3797, 2015, https://doi.org/10.1007/s12517-014-1409-8.

SBAA, S., HOLLENDER, F., PERRON, V., IMTIAZ, A., BARD, P.-Y., MARISCAL, A., COCHARD, A., DUJARDIN, A. Analysis of rotation sensor data from the SINAPS@ Kefalonia (Greece) post-seismic experiment—link to surface geology and wavefield characteristics. *Earth Planets Space*, 2017 (69), 124, 1–19, 2017, https://doi.org/10.1186/s40623017-0711-6.

STUPAZZINI, M., DE LA PUENTE, J., SMERZINI, C., KÄSER, M., IGEL, H., CASTELLANI, A. Study of Rotational Ground Motion in the Near-Field Region. *Bull. Seismol. Soc. Am.*, 99, (2B). 1271–1286, 2009, https://doi.org/10.1785/0120080153.

TAKEO, M. Rotational motions observed during an earthquake swarmin April 1998 offshore Ito, Japan. *Bull Seismol Soc Am.*, 99, (2B), 1457–1467, 2009, https://doi.org/10.1785/0120080173.

TEPER, L. Geometry of fold arrays in the Silesian-Cracovian region of southern Poland, in: Cosgrove, J.W., Ameen, M.S. (Eds.), Forced Folds and Fractures. *Geological Society, London*, Special Publications, London, 2000, 169, 167–179. https://doi.org/10.1144/gsl.sp.2000.169.01.12.

WANG, H., IGEL, H., GALLOVIČ, F., COCHARD, A. Source and Basin Effects on Rotational Ground Motions: Comparison with Translations. *Bull Seismol Soc Am.*, 99 (2B), 1162–1173, 2009, https://doi.org/10.1785/0120080115.

YIN, J., NIGBOR, R. L., CHEN, Q., STEIDL, J. Engineering analysis of measured rotational ground motions at GVDA. *Soil Dyn. Earthq. Eng.*, 87, 125-137, 2016, http://dx.doi.org/10.1016/j.soildyn.2016.05.007.

ZEMBATY, Z. Deriving seismic surface rotations for engineering purposes. In: Teisseyre, R., Takeo, M., Majewski, E. (Eds), Earthquake Source Asymmetry, Structural Media and Rotation Effects, *Springer*, Berlin, Heidelberg, 2006, 549-568.

ZEMBATY, Z., MUTKE, G., NAWROCKI, D., BOBRA, P. Rotational ground-motion records from induced seismic events. *Seismol. Res. Lett.*, 88 (1), 13-22, 2017, https://doi.org/10.1785/0220160131.

Authors

[1] University of Silesia in Katowice, Faculty of Natural Sciences, Bedzinska 60, Sosnowiec, Poland